

Full Length Research Paper

Sliding mode control applied to a photovoltaic water-pumping system

Mahmoud Ellouze^{1,2}, Riadh Gamoudi¹ and Abdelkader Mami^{1,3}

¹Laboratory of Analysis and Control Systems (LACS), ENIT, Tunis, C. U. Belvedere 1060, Tunis, Tunisia.

²Superior Institute of Technology and Data Processing, 2080 Ariana, Tunisia.

³Department of Physics, Faculty of Sciences of Tunis, Electronic Laboratory, 2092 El Manar, Tunis, Tunisia.

Accepted 18 February 2010

In this paper, a nonlinear control of an induction motor (IM) supplied with a photovoltaic generator to assure the level control of two coupled tanks is designed. The global system is decomposed into two separate models thus, coupled are assured by discontinuous command. In the first step, we propose a sliding mode technique to make the speed and the flux control of the IM robust to parameter variations. Then, the aim is to assure the stability of the system autonomously towards a desired state (water level), by varying the speed of the IM. The use of the nonlinear sliding mode method provides a very good performance for motor operation and robustness of the control law despite the external/internal perturbation. Simulation results are given to highlight the performance of the proposed control technique under load disturbances and parameter uncertainties.

Key words: Sliding mode control, photovoltaic energy, water level, coupled reservoirs, induction motor-pump.

INTRODUCTION

The sliding mode controller is designed for a class of non linear dynamic systems to tackle the problems with model uncertainties, parameter fluctuations and external disturbances. By this design, the bounds of the uncertainties are not required to be known in advance.

The variable structure control (VSC) possesses this robustness using the sliding mode control that can offer many good properties such as good performance against unmodelled dynamics, insensitivity to parameter variation, external disturbance rejection and fast dynamic (Utkin, 1977). These advantages of sliding mode control can be employed in the position and speed control of an alternative current system.

In this paper, we begin with the IM oriented model in view of the vector control, next the rotor flux Φ_r , is estimated. We, then, present the sliding mode theory and design the sliding mode controllers of rotor flux and motor speed. Finally, we provide some conclusion remarks on the control proposed of IM using sliding mode.

The induction machine is largely used in industry, mainly

due to its reliability and relatively low cost. The control of the induction machine (IM) must take into account machine specificities: the high order of the model, the nonlinear functioning as well as the coupling between the different variables of control.

In the second stage, we are interested in the level control in the coupled tanks. Several researchers have investigated the problem of controlling liquid flow of a single or multiple tanks (Khan and Spurgeon, 2006; Pan et al., 2005). The speed variations of the IM carry the level regulation control, the relation between speed and the flow of pumped water is given by (Caro and Bonal, 1997).

PROCESS DESCRIPTION

The increasing demand of water in rural zones and isolated sites made that a growing interest is done to the utilization of photovoltaic (PV) generator as energy source for several motor-pumps. In fact, the realization of autonomous, reliable pumping systems with a good efficiency, gives a practical and economical solution to the water lack problem in desert regions (Dhafer et al.,

*Corresponding author. E-mail: riadh.gamoudi@gmail.com.

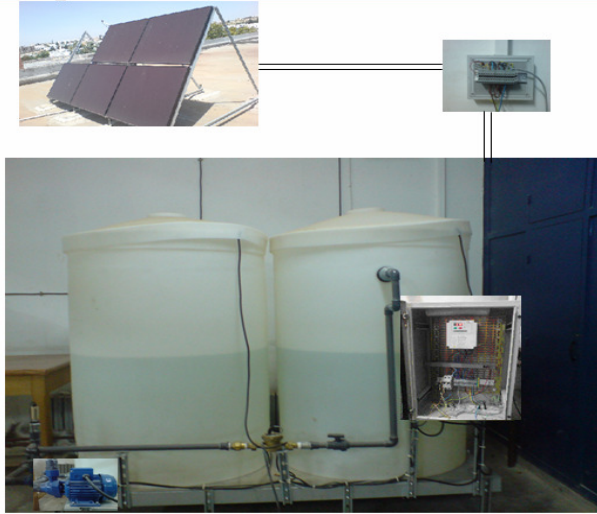


Figure 1. Scheme of the global process.

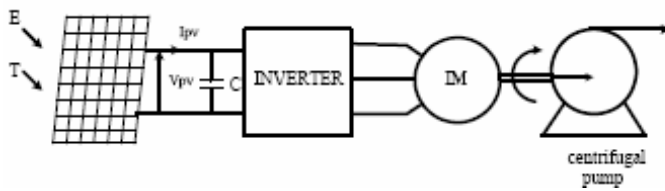


Figure 2. Diagram of the photovoltaic water-pumping system.

2007). For this reason, we chose the system in (Figure 1) to study its feasibility in real case.

The system under study is a combination of two subsystems. The PV-powered water pumping system investigated in this paper consists mainly of a PV generator, DC-AC converter, and induction motor-pump. The second subsystem is composed of two coupled tanks.

DYNAMIC MODEL OF INDUCTION MOTOR

The first part of the global system investigated in this article consists mainly of a photovoltaic generator (PV), a three phase inverter MLI, and an induction motor-pump. The scheme of the studied process is indicated in (Figure 2).

We suppose, the inverter behaves as a perfect transferring power organ. Similarly, the characteristic of the generator PV is supposed ideal that we can assimilate in a classic power source. The photovoltaic generator is characterized (at an illumination of $1000W/m^2$), by an opened circuit voltage $V_{co} = 471V$, an optimal operation point M (378 V; 2,27 A) and $I_{pH} = 2.47A$ $I_s = 8.143 \times 10^{-6} A$, $V_T = 37.5V$ (Figure 3). Afterward, we use the equivalent model of a three-phase

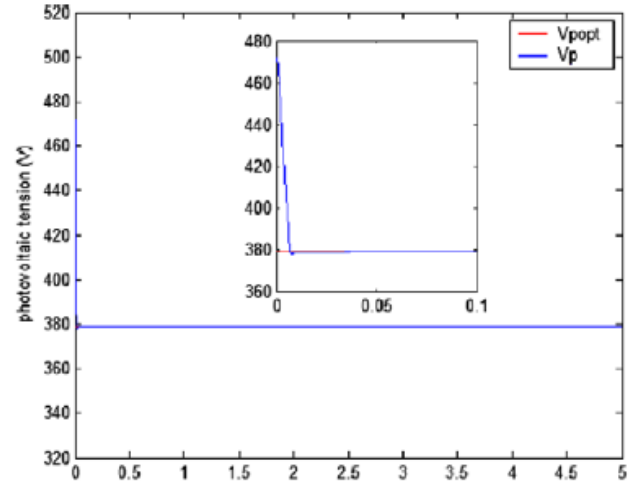


Figure 3. Simulation responses of the PV in closed loop.

asynchronous motor in the Park transformation (Olorunfemi, 1991; Mimouni et al., 2004).

So, an induction machine model can be described by the following state equations in the synchronous reference frame whose axis d is aligned with the rotor flux vector.

$$(\Phi_{rq} = 0): \frac{di_{ds}}{dt} = -\gamma_{ds} + \omega_s i_{qs} + \frac{K}{T_r} \Phi_{rd} + \frac{1}{\delta L_s} u_{ds} \quad (1)$$

$$\frac{di_{qs}}{dt} = -\omega_s i_{ds} - \gamma_{qs} - p\Omega K \Phi_{rd} + \frac{1}{\delta L_s} u_{qs} \quad (2)$$

$$\frac{d\Phi_{rd}}{dt} = \frac{M_{sr}}{T_r} i_{ds} - \frac{1}{T_r} \Phi_{rd} \quad (3)$$

$$\frac{d\Phi_{rq}}{dt} = \frac{M_{sr}}{T_r} i_{qs} - (\omega_s - p\Omega) \Phi_{rd} \quad (4)$$

$$\frac{d\Omega}{dt} = \frac{pM_{sr}}{JL_r} (\Phi_{rd} i_{qs}) - \frac{f}{J} \Omega - \frac{1}{J} C_r \quad (5)$$

With:

$$T_r = \frac{L_r}{R_r}, \quad \delta = 1 - \frac{M_{sr}^2}{L_s L_r}, \quad K = \frac{M_{sr}}{\delta L_s L_r},$$

$$\gamma = \frac{R_s}{\delta L_s} + \frac{R_r M_{sr}^2}{\delta L_s L_r^2}$$

Where the electromagnetic torque is given in d-q frame:

$$C_{em} = p \frac{M_{sr}}{L_r} (\Phi_{rd} i_{qs}) \quad (6)$$

Where Φ_{rd}, Φ_{rq} are rotor flux components, u_{sd}, u_{sq} are stator voltage components, i_{ds}, i_{qs} are stator current components, δ is leakage factor and p is number of pole pairs. R_s and R_r are stator and rotor resistances, L_s and L_r denote stator and rotor inductances, whereas M_{sr} is mutual inductance. C_{em} is the electromagnetic torque, C_r is the load torque, J is the moment of inertia of the Induction Motor, Ω is mechanical speed, ω_s is stator pulsation, f is damping coefficient, T_r is rotoric time-constant.

SLIDING MODE CONTROL DESIGN

Consider a nonlinear system which can be represented by the following state space model in a canonical form (Slotine and Li, 1998):

$$\begin{aligned} \dot{x}^{(n)}(t) &= f(x(t), t) + g(x(t), t)u + d(t) \\ y(t) &= x(t) \end{aligned} \quad (7)$$

Where $x = [x(t) \dot{x}(t) \dots x^{(n-1)}(t)]^T$ is the state vector, $f(x(t), t)$ and $g(x(t), t)$ are nonlinear functions, u is the control input, $d(t)$ is the external disturbances.

The objective of the control is to determine a control law $u(t)$ to force the system output $y(t)$ in (7) to follow a given bounded reference signal $y_d(t)$, that is, the tracking error $e(t) = y_d(t) - y(t)$ and its forward shifted values, defined as:

$$\begin{aligned} e^{(i)}(t) &= y_d^{(i)}(t) - y^{(i)}(t) \\ &= x_d^{(i)}(t) - x^{(i)}(t), \quad (i=1, \dots, n-1) \end{aligned} \quad (8)$$

The design of SMC involves two tasks. The first one is to select the switching hyperplane to prescribe the desired dynamic characteristics of the controlled system. The second one is to design the discontinuous control such that the system enters the sliding mode $s(x, t) = 0$ and remains in it forever (Slotine and Li, 1998).

In this paper, we use the sliding surface proposed par J.J. Slotine,

$$s(x, t) = \left(\frac{d}{dt} + \lambda \right)^{n-1} e(t) \quad (9)$$

In which $e = x_d(t) - x(t)$, λ is a positive coefficient, and n is the system order.

It remains to be shown that the control law can be constructed so that the sliding surface will be reached. The surfaces are chosen as functions of the error between the references input signal and the measured signals (Utkin, 1993).

Then, a sliding hyperplane can be represented as $s(x, t) = 0$.

Consider a Lyapunov function:

$$V = \frac{1}{2} s^2 \quad (10)$$

From Lyapunov theorem we know that if \dot{V} is negative definite, the system trajectory will be driven and attracted toward the sliding surface and remain sliding on it until the origin is reached asymptotically (Buhler, 1986).

$$\dot{V} = s \dot{s} \quad (11)$$

The simplified 1st order problem of keeping the scalar $s(x, t)$ at zero can be achieved by choosing the control law $u(t)$. A sufficient condition for the stability of the system is

$$\frac{1}{2} \frac{d}{dt} s^2 \leq -\eta |s| \quad (12)$$

Where η is a positive constant.

The equation (12) is called reaching condition or sliding condition. $s(t)$ verifying (12) is referred to as sliding surface, and the system's behaviour once on the surface is called sliding mode.

If the control input is so designed that the inequality (12) is satisfied, together with the properly chosen sliding hyperplane, the state will be driven toward the origin of the state space along the sliding hyperplane from any given initial state. This is the way of the SMC that guarantees asymptotic stability of the systems.

The process of sliding mode control can be divided in two phases, that is, the approaching phase and the sliding phase. The sliding mode control law $u(t)$ consists of two terms, equivalent term $u^{eq}(t)$, and switching term $u^s(t)$.

In the sliding phase, where $s(x, t) = 0$ and $\dot{s}(x, t) = 0$ the equivalent term $u^{eq}(t)$ is designed to keep the system on the sliding surface. In the approaching phase, where $s(x, t) \neq 0$, the switching term $u^s(t)$ is designed to satisfy the reaching condition (12). While in sliding phase we have:

$$\dot{s}(x, t) = 0 \quad (13)$$

By solving the above equation formally for the control input, we obtain an expression for u called the equivalent control $u^{eq}(t)$, which can be interpreted as the continuous control law that would maintain $\dot{s}(x,t)=0$ if the dynamics were exactly known.

In order to satisfy sliding conditions (12) and to despite uncertainties on the dynamic of the system, we add a discontinuous term across the surface $s(x,t)=0$, so the sliding mode control law $u(t)$ has the following form:

$$\begin{aligned} u &= u^{eq} + u^s \\ u^s &= -K \operatorname{sgn}(s(x,t)) \end{aligned} \quad (14)$$

Where K is the control gain.

For a defined function φ :

$$\operatorname{sgn}(\varphi) = \begin{cases} 1, & \text{if } \varphi > 0 \\ 0, & \text{if } \varphi = 0 \\ -1, & \text{if } \varphi < 0 \end{cases} \quad (15)$$

The controller described by the equation (14) presents high robustness, insensitive to parameter fluctuations and disturbances (Utkin, 1977; Slotine and Li, 1998; Utkin, 1978; Khalil, 1992), but it will have high-frequency switching (chattering phenomena) near the sliding surface due to sgn function involved. These drastic changes of input can be avoided by introducing a boundary layer with width ε (Slotine and Li, 1998; Khalil, 1992). Thus replacing $\operatorname{sgn}(s(t))$ by $\operatorname{sat}(s(t)/\varepsilon)$ in (14), we have

$$u = u^{eq} - K \operatorname{sat}(s(x,t)) \quad (16)$$

Where

$$\begin{aligned} \varepsilon &> 0 \\ \operatorname{sat}(\varphi) &= \begin{cases} \operatorname{sgn}(\varphi) & \text{if } |\varphi| \geq 1 \\ \varphi & \text{if } |\varphi| < 1 \end{cases} \end{aligned}$$

After this step, the objective is to determine a control law which drives the state trajectories along the surface.

Speed control

To control the speed of the induction machine, three surfaces are chosen. Variables of control are the rotation speed Ω and the flux Φ_{rd} . The flux will be maintained at its nominal value to have a maximal torque.

We take $n=1$, the speed control manifold equations can be obtained as:

$$\begin{aligned} S(\Omega) &= \Omega_{ref} - \Omega \\ \dot{S}(\Omega) &= \dot{\Omega}_{ref} - \dot{\Omega} \end{aligned} \quad (17a)$$

Substituting the expression of $\dot{\Omega}$ equation (5) in equation (17a), we obtain:

$$\dot{S}(\Omega) = \dot{\Omega}_{ref} - \left[\frac{pM_{sr}}{JL_r} (\Phi_{rd} i_{qs}) - \frac{f}{J} \Omega - \frac{1}{J} C_r \right] \quad (17b)$$

We take

$$i_{qs} = i_{qs}^{eq} + i_{qs}^s \quad (17c)$$

During the sliding mode and in permanent regime, we have:

$$S(\Omega) = 0, \quad \dot{S}(\Omega) = 0, \quad i_{qs}^s = 0 \quad (17d)$$

Where the equivalent control is:

$$i_{qs}^{eq} = \frac{JL_r}{pM_{sr}\Phi_{rd}} \left(\dot{\Omega}_{ref} + \frac{f}{J} \Omega + \frac{C_r}{J} \right) \quad (17e)$$

During the convergence mode, the condition $S(\Omega) \dot{S}(\Omega) \leq 0$ must be verified. We obtain:

$$\dot{S}(\Omega) = -\frac{p^2 M_{sr} \Phi_{rd}}{JL_r} i_{qs}^s \quad (17f)$$

Therefore, the correction factor is given by:

$$i_{qs}^s = -k_{\Omega} \cdot \operatorname{sat}(S(\Omega)) \quad (17g)$$

To verify the system stability condition, the parameter k_{Ω} must be positive.

Stator current control and limitation

In order to limit all possible overshoot of the current i_{qs} , we add a limiter of current defined by

$$i_{qs}^{\lim} = i_{qs}^{\max} \cdot \operatorname{sat}(i_{qs}) \quad (18a)$$

The current control manifold is

$$\begin{aligned} S(i_{qs}) &= i_{qs}^{\lim} - i_{qs} \\ \dot{S}(i_{qs}) &= \dot{i}_{qs}^{\lim} - \dot{i}_{qs} \end{aligned} \quad (18b)$$

Substituting the expression of \dot{i}_{qs} Equation (2) in Equation

(18 b), we obtain:

$$\dot{S}(i_{qs}) = i_{qs} \lim - \left(-\omega_s i_{ds} - \gamma_{qs} - p\Omega K\Phi_{rd} + \frac{1}{\mathcal{L}_s} u_{qs} \right) \quad (18c)$$

The control voltage is

$$u_{qs}^{ref} = u_{qs}^{eq} + u_{qs}^s \quad (18d)$$

$$u_{qs}^{eq} = \mathcal{L}_s \left(i_{qs} \lim + \omega_s i_{ds} + \gamma_{qs} + p\Omega K\Phi_{rd} \right) \quad (18e)$$

$$u_{qs}^s = -k_{i_{qs}} \cdot sat \left(S(i_{qs}) \right) \quad (18f)$$

To verify the system stability condition, the parameter $k_{i_{qs}}$ must be positive.

Flux control

In the proposed control, we take n=2 to appear control u_{ds}^{ref} , the manifold equation can be obtained by:

$$\begin{aligned} S(\Phi_{rd}) &= \lambda (\Phi_{rd}^{ref} - \Phi_{rd}) + (\dot{\Phi}_{rd}^{ref} - \dot{\Phi}_{rd}) \\ \dot{S}(\Phi_{rd}) &= \lambda (\dot{\Phi}_{rd}^{ref} - \dot{\Phi}_{rd}) + (\ddot{\Phi}_{rd}^{ref} - \ddot{\Phi}_{rd}) \end{aligned} \quad (19a)$$

The control voltage is

$$u_{ds}^{ref} = u_{ds}^{eq} + u_{ds}^s \quad (19b)$$

$$u_{ds}^{eq} = \mathcal{L}_s \left(\left(\ddot{\Phi}_{rd}^{ref} + \lambda \dot{\Phi}_{rd}^{ref} + \left(\frac{1}{T_r} - \lambda \right) \dot{\Phi}_{rd} \right) \frac{T_r}{M_{sr}} \right) \quad (19c)$$

$$\left(-\gamma_{i_{ds}} + \omega_s i_{qs} + \frac{K}{T_r} \Phi_{rd} \right)$$

$$u_{ds}^s = -k_{\Phi_{rd}} \cdot sat \left(S(\Phi_{rd}) \right) \quad (19d)$$

To verify the system stability condition, the parameter $k_{\Phi_{rd}}$ must be positive.

The selection of coefficients k_{Ω} , $k_{i_{qs}}$, $k_{\Phi_{rd}}$ and λ must be done in order to satisfy following requirements:

Existence condition of the sliding mode, which requires that the state trajectories are directed toward the sliding manifold,
 Hitting condition, which requires that the system trajectories encounter the manifold sliding irrespective of

their starting point in the state space (insure the rapidity of the convergence),

Stability of the system trajectories on the sliding manifold,

Not saturate the control to allow the application of the control discontinuous.

DYNAMIC MODEL OF HYDRAULIC SYSTEM

The second part of the global procedure is formed by a coupled tank, considered as a benchmark for the study and the analysis command of hydraulic systems. This device, allows to examine the law order in the liquid level reservoirs, while varying the debit from the variation of the speed of the pump.

This process behaves two vertical tanks coupled by a flow canal, a manual valve used to change the canal section, in consequently, to change the characteristics of flow between the reservoirs (Figure 4). A level sensor is installed in the top of every reservoir. The relation between the speed of the IM Ω and the entry debit of the second reservoir q_2 :

$$q_2 = a_1 \cdot a_2 \cdot G_p \cdot \Omega \quad (20a)$$

The second reservoir can be filled from the first reservoir by the intermediary of canal 1. While, the debit of the second reservoir towards the first is assured by canal 2. The equilibrated equation of the flow, for the first reservoir:

$$\dot{h}_1 = \frac{1}{S} (q_{21} - q_1) \quad (20b)$$

For the second reservoir:

$$\dot{h}_2 = \frac{1}{S} (q_2 - q_{21}) \quad (20c)$$

Such as:

$$q_1 = s_1 \cdot \sqrt{2gh_1} \quad (20d)$$

$$q_{21} = s_2 \cdot a_0 \sqrt{2g(h_2 - h_1)} \quad (20e)$$

With:

- h_1 : the level in the first tank
- h_2 : the level in the second tank,
- q_1 : the inlet flow rate,
- q_2 : the flow rate from Tank 1 - Tank 2,
- q_{12} : the flow rate out of Tank 2,
- g : the gravitational constant,
- S : the cross-section area of Tank 1 and Tank 2,

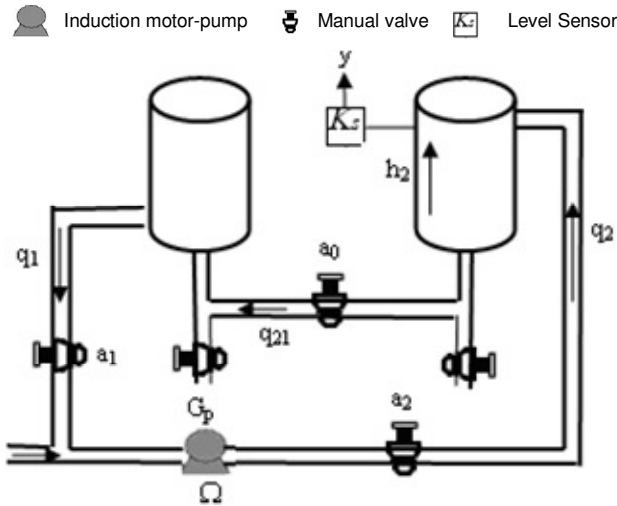


Figure 4. Descriptive scheme of hydraulic system.

s_1, s_2 the area of the coupling orifice,
 a_1, a_2 the coefficients of the manual valve 1 and valve 2,
 a_0 the offloads coefficient valve 3,
 G_p : the pump gain

Finally, the hydraulic system is governed by the following non linear differential equation:

$$\begin{cases} \frac{dh_1}{dt} = \frac{1}{S} (s_2 a_0 \sqrt{2g(h_2 - h_1)} - s_1 \sqrt{2gh_1}) \\ \frac{dh_2}{dt} = \frac{1}{S} (a_1 a_2 G_p \Omega - s_2 a_0 \sqrt{2g(h_2 - h_1)}) \\ y = K_s h_2 \end{cases} \quad (20f)$$

K_s : the level sensor gain.

The centrifugal pump is also described by characteristic $H(Q)$ given by (Caro and Bonal, 1997):

$$b_0 \Omega_m^2 + b_1 \Omega_m Q + b_2 Q^2 = H_p + X Q^2 \quad (20g)$$

Where b_0, b_1, b_2 and X are constant parameters. H_p and Q are respectively the geometric head and the flow of pumped water.

In the model of Figure 4, Ω_{min} being the minimal speed from which the pump starts to generate a pumped water flow. It is given by the following relation (Caro and Bonal, 1997):

$$\Omega_{min} = \sqrt{\frac{-4(b_2 - X)H_p}{b_1^2 - 4(b_2 - X)b_0}} \quad (20h)$$

Three cases are possible:

If $\Omega < \Omega_{min}$ no flow rate is generated:

$$Q = 0 \quad (20i)$$

If $\Omega = \Omega_{min}$ the pump starting to pumped water:

$$Q = Q_{min} = \frac{b_1 \Omega_{min}}{2(b_2 - X)} \quad (20j)$$

If $\Omega > \Omega_{min}$ the flow pumped water is given by:

$$Q = \frac{-b_1 \Omega - \sqrt{(b_1 \Omega)^2 - 4(b_2 - X)(b_0 \Omega^2 - H_p)}}{2(b_2 - X)} \quad (20k)$$

MLI TENSION INVERTER

The technique of the natural modulation permits to determine the moments and the durations of the switches lighting or extinction by comparison between the tension references and a triangular high frequency carry. The three-phase tensions (with MLI control) provided by the inverter (Figure 5) are given according to the states of the switches T_{ci} and of the direct tension U_c by:

$$\begin{bmatrix} V_A \\ V_B \\ V_C \end{bmatrix} = \frac{1}{3} \begin{bmatrix} 2 & -1 & -1 \\ -1 & 2 & -1 \\ -1 & -1 & 2 \end{bmatrix} \begin{bmatrix} F_{11} \\ F_{21} \\ F_{31} \end{bmatrix} U_c \quad (21)$$

Where the logical function connexion F_{c1} is defined as: $F_{c1} = 1$ if the switch T_{c1} is closed, $F_{c1} = 0$ if the switch T_{c1} is opened.

The switch T_{ci} ($c \in \{1, 2, 3\}, i \in \{1, 2\}$) is supposed perfect. The simple inverter voltage can be presented by logical function connexion in matrix from as (Equation 21).

The tension curve of the voltage inverter is given in (Figure 6).

DESCRIPTION OF THE SYSTEM

The bloc diagram of the proposed robust control scheme is presented in (Figure 7). The blocks SMC1, SMC2, SMC3, and SMC4 represent the proposed sliding mode controllers. To avoid the appearance of an inaccurate value of current, a saturation bloc is used.

The rotor flux Φ_r is estimated by the "flux rotor observer". The block 'IM' represents the induction motor. We implement the previous sliding mode algorithms using a MATLAB/Simulink simulator.

SIMULATION RESULTS

In order to validate the control strategies as discussed above, we have studied the speed performances with

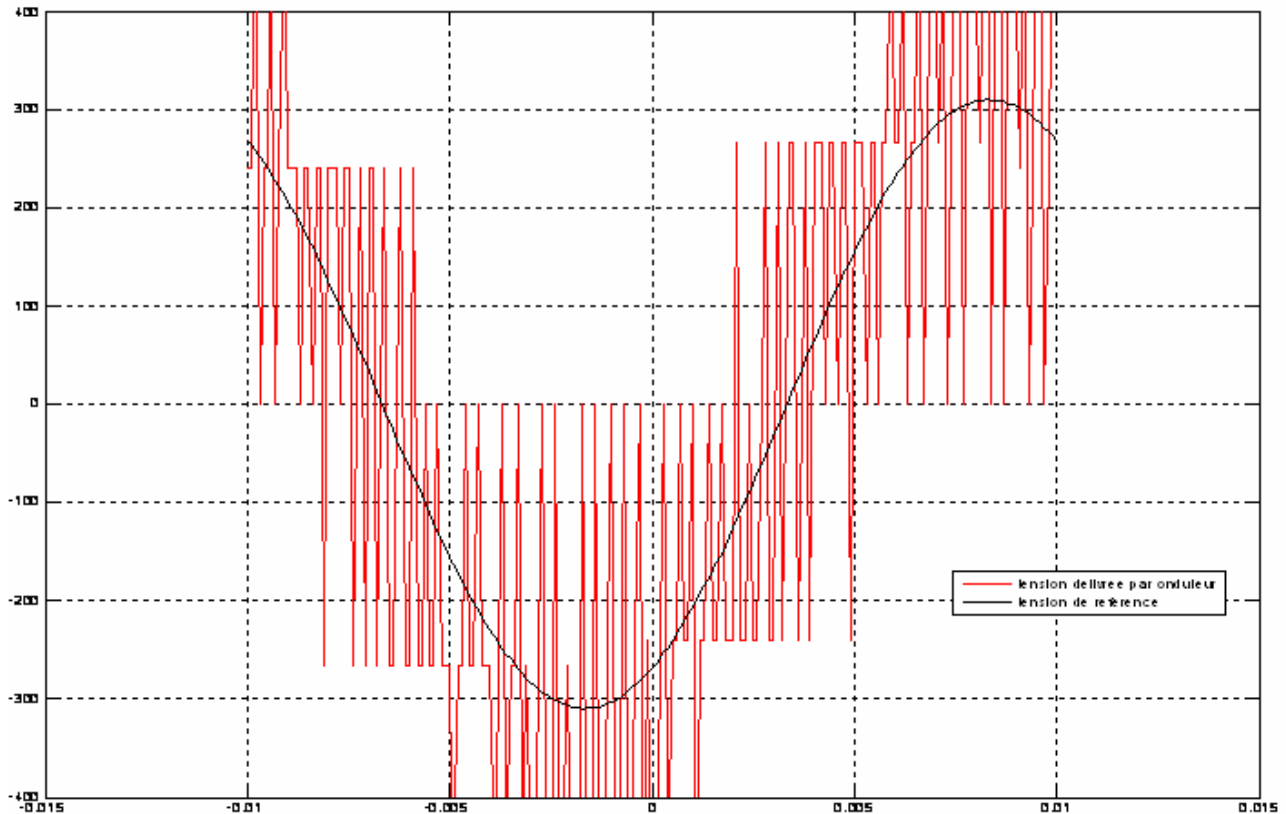


Figure 6. Input logical signals MLI for the switching frequency inverter.

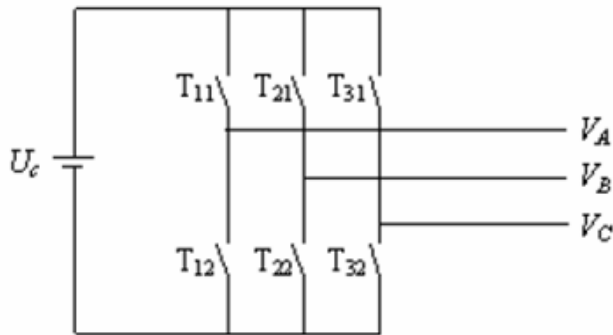


Figure 5. Voltage inverter.

current limitation described in (Figure 7). The feedback control algorithms were iterated until best simulation results were obtained. (Figure 9) shows the robustness tests in relation to inertia variations. (Figure 10) shows the robustness tests to the stator and rotor resistance variations.

The speed and flux references are respectively (Figure 8):

$$\Omega_{ref} = 100rd / s = 960rpm, \quad \Phi_{r0} = 0.6wb$$

In the second part of the global system, the bloc SMC4 permits to find out the pursuit of the liquid level in the second tank (Figure 11). (Figure 12) shows the robustness tests in relation to inertia variations (Figure 13) shows the robustness tests to the stator and rotor resistance variations.

The SMC4 law (Figure 14) is given by:

$$S(h_2) = h_{2ref} - h_2 \tag{22a}$$

$$u = u^{eq} + u^s \tag{22b}$$

Where

$$u^{eq} = \frac{S}{a_1 \cdot a_2 \cdot G_p} \cdot \dot{h}_{2ref} + \frac{s_2 \cdot a_0}{a_1 \cdot a_2 \cdot G_p} \cdot \sqrt{2 \cdot g} \cdot \sqrt{h_2 - h_1}$$

$$u^s = -K' \cdot \text{sat}(S(h_2)) \tag{22c}$$

K' a positive constant

Variation effect of rotor time constant

The influence on variation rotor time constant is an important

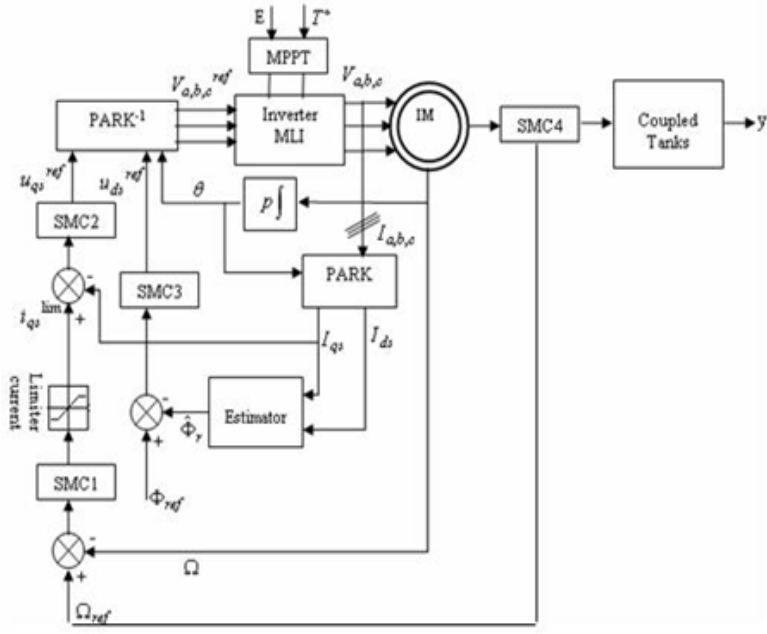


Figure 7. Block diagram of the proposed control scheme of IM coupled in hydraulic system using the sliding mode controllers.

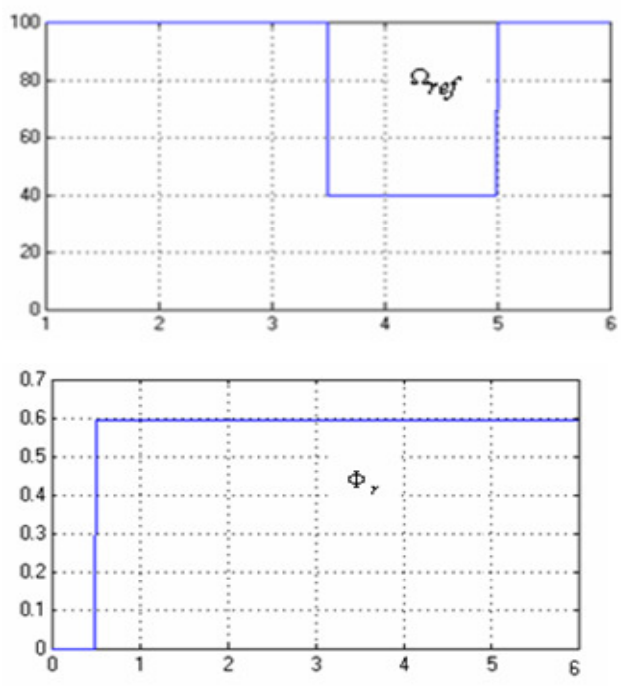


Figure 8. Reference of speed, and rotor flux.

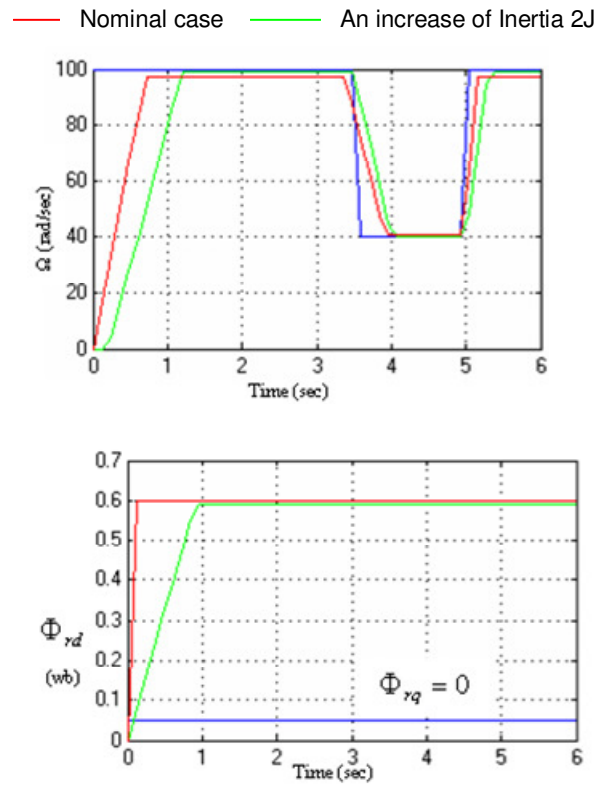


Figure 9. System responses.

parameter for studying the dynamic response and robustness of the controller, particularly for the system stability. Several research tasks (Jeon et al., 2002), showed that the performances of the control with (VSC) depend strongly on the accuracy with which the parameters of the

motor are known exactly. Thus, for rated values of the command currents. The simulation of mathematical

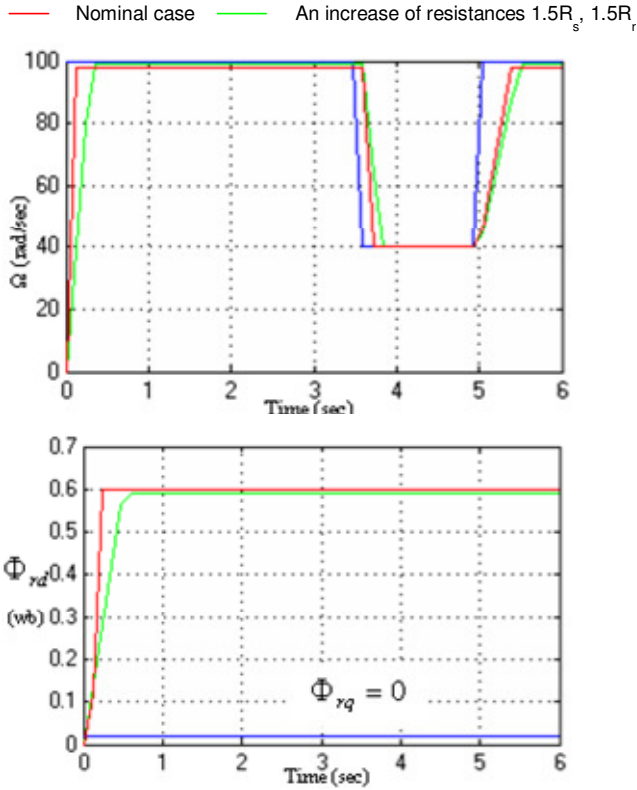


Figure 10. System responses

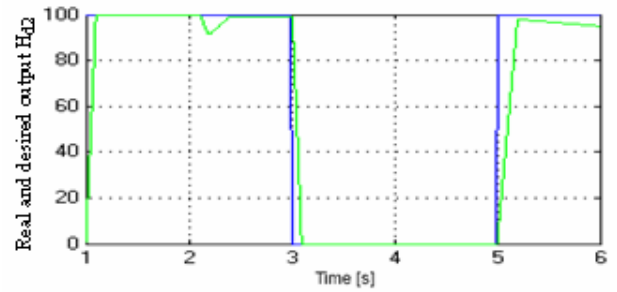


Figure 12. Real and desired output H_{d2} , case an increase of Inertia $2J$.

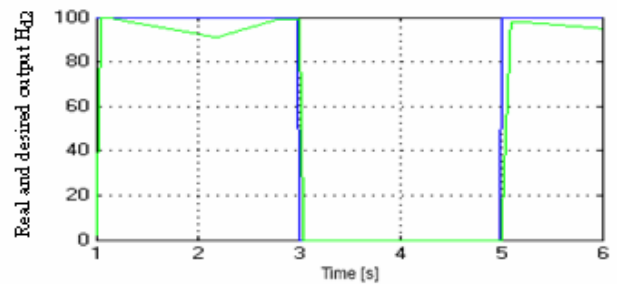


Figure 13. Real and desired output H_{d2} , case an increase resistances $1.5R_s, 1.5R_r$.

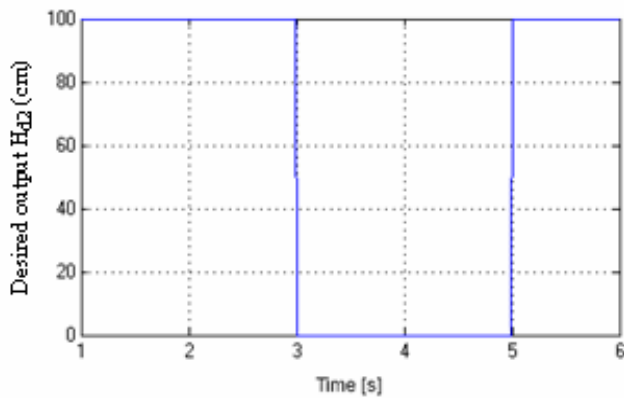


Figure 11. Reference level in the second tank.

equations given by (23a) and (23b) are plotted in (Figure 15).

$$\frac{C_{em}}{C_{em}^*} = \frac{T_r}{T_r^*} \frac{1 + \left(\frac{i_{qs}^*}{i_{ds}^*}\right)^2}{1 + \left[\left(\frac{T_r}{T_r^*}\right)\left(\frac{i_{qs}^*}{i_{ds}^*}\right)\right]^2} \quad (23a)$$

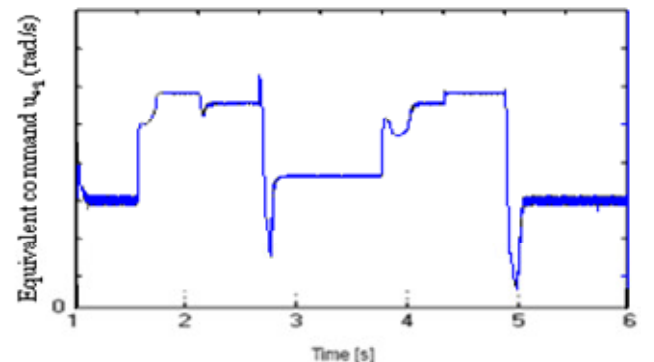
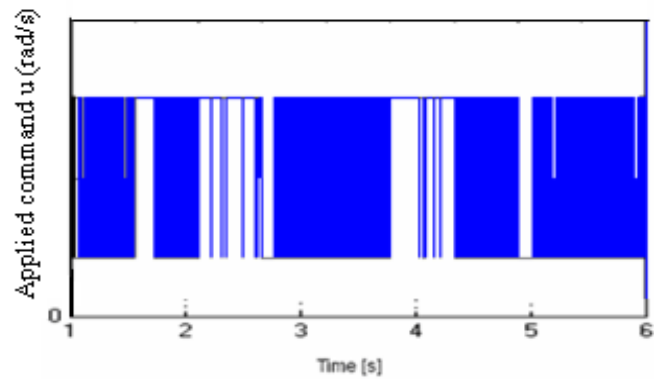


Figure 14. Command applied to the entry of the hydraulic system.

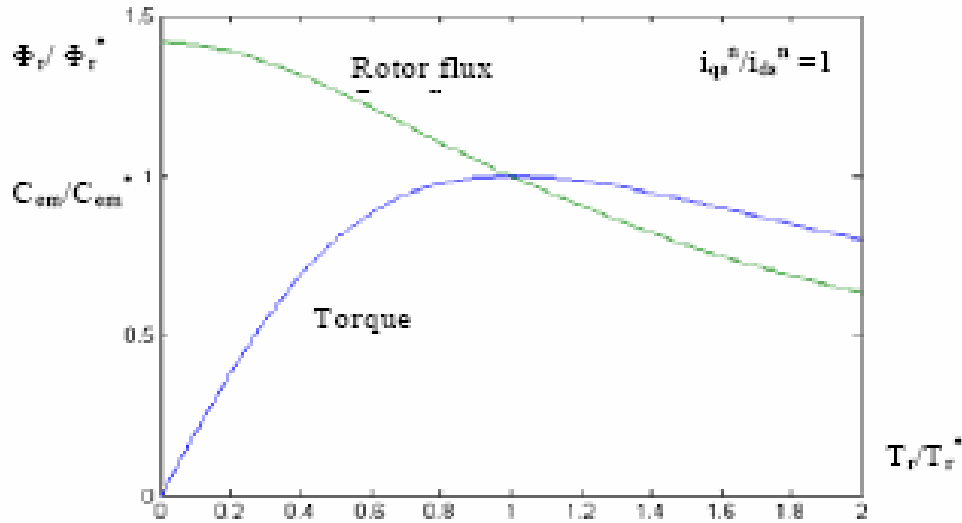


Figure 15. Curves of steady-state effect parameters for rate flux and torque currents command.

$$\frac{\phi_r}{\phi_r^*} = \frac{\sqrt{1 + \left(\frac{i_{qs}^*}{i_{ds}^*}\right)^2}}{\sqrt{1 + \left[\left(\frac{T_r}{T_r^*}\right)\left(\frac{i_{qs}^*}{i_{ds}^*}\right)\right]^2}} \quad (23b)$$

C_{em}^* and ϕ_r^* are respectively reference of the electromagnetic torque and the rotor flux.

These curves show that the actual value of the rotor time constant is smaller than the predicted value when $\frac{T_r}{T_r^*} < 1$.

The identification method of rotor time constant is studied and simulated.

CONCLUSION

A sliding mode control method has been proposed and used for the control of an induction machine. It has shown the robustness of proposed control. The speed control operates with enough stability and has strong robustness to parameter variations.

The control of two coupled tanks is assured by the speed variation. The performances of the controlled system are studied under variations in system parameters and in the presence of external disturbance. The simulation results indicate that the proposed control schemes work very well and are robust to change in the parameters of the system as well as to disturbances acting on the global system.

Furthermore, this regulation presents a simple robust control algorithm that has the advantage to be easily implantable in calculator.

REFERENCES

Buhler H (1986). Réglage par mode de glissement, Presses polytechniques romandes, Lausanne.
 Caro JM, Bonal J (1997). Entraînements Electriques à Vitesse Variable. Lavoisier, vol. (1).
 Dhafer M, Andoulsi R, Mami A, Dauphin-Tanguy G (2007). Bond graph modelling of a photovoltaic system feeding an induction motor-pump. Simulation Modelling Practice and Theory, (Elsevier), 15: 1224–1238.
 Jeon SH, Oh KK, Choi JY (2002). Flux observer with on line tuning of stator and rotor resistance for induction motors. IEEE Trans. Ind. Electron. 49: 653-664.
 Khalil HK (1992). Non linear system, New York: MacMillan.
 Khan MK, Spurgeon SK (2006). Robust MIMO water level control in interconnected twin-tanks using second order sliding mode control. Contr. Eng. Practice, 14: 375–86.
 Mimouni MF, Mansouri MN, Benghanem B, Annabi M (2004). Vectorial command of an asynchronous motor fed by a photovoltaic generator. Renewable Energy, 29: 433-442.
 Olorunfemi O (1991). Analysis of current source induction motor drive fed from photovoltaic energy source. IEEE Trans. on Energy Conversion, 6(6): 99-106.
 Pan H, Wong H, Kapila V, Queiroz MS (2005). Experimental validation of a nonlinear backstepping liquid level controller for a state coupled two tank system. Contr. Eng. Practice, 13: 27–40.
 Slotine JJE, Li W (1998). Applied nonlinear control, USA: Prentice-Hall.
 Utkin VI (1977). Variable structure systems with sliding modes. IEEE Trans. Automat. Contr., 2(22): 212-222.
 Utkin VI (1978). Sliding modes and their application in variable structure system. Moscow: MIR.
 Utkin VI (1993). Sliding mode control design principles and applications to electric drives. IEEE Trans. Ind. electronic, 40: 23-36.

APPENDIX**Motor parameters**

Nominal power output $P = 750 \text{ W}$
 Nominal voltage: 220V
 Nominal current: 1.6 A
 Number of pole pairs: $p = 2$
 Rotoric resistance: $R_r = 0.79 \Omega$
 Statoric resistance: $R_s = 1.47 \Omega$
 Rotoric cyclic inductance $L_r = 0.094 \text{ H}$
 Statoric cyclic inductance $L_s = 0.105 \text{ H}$
 Mutual cyclic inductance $M_{sr} = 0.094 \text{ H}$
 Moment of inertia $J = 0.00256 \text{ Kgm}^2$
 Friction coefficient $f = 0.0029 \text{ Kgm}^2\text{s}^{-1}$

Pump parameters

Geometric head $H_p = 0.1 \text{ m}$
 $b_0 = 1.61 \cdot 10^{-4} \text{ m s}^2 \text{ rd}^{-2}$
 $b_1 = 2.584 \cdot 10^{-3} \text{ m s}^2 \text{ l}^{-1} \text{ rd}^{-1}$
 $b_2 = -0.49 \text{ m l}^2 \text{ s}^{-2}$
 $X = 0.98388 \text{ m s l}^{-1}$

Coupled reservoirs

The cross-section area of Tanks: $S = 1.1310 \text{ m}^2$
 The area of the coupling orifices $s_1, s_2 = 0.0079 \text{ m}^2$
 The coefficients of the manual valves $a_1, a_2, a_0 \sim 1$
 The pump gain $G_p = 7.5 \text{ m}^3 \cdot \text{s}^{-1} \cdot \text{v}^{-1}$
 The level sensor gain $K_s = 24.5 \text{ v} \cdot \text{m}^{-1}$
 The gravitational constant $g = 9.8 \text{ m} \cdot \text{s}^{-2}$